European Conference on Optical Communication (ECOC) 2022 © Optica Publishing Group 2022

Mitigation of Anomaly Loss in Optical Transmission System with Hybrid EDFA/Raman Amplification

Inwoong Kim, Olga Vassilieva, Paparao Palacharla

Fujitsu Network Communications, 2801 Telecom Parkway, Richardson, TX 75082, USA, inwoong.kim@fujitsu.com

Abstract *We analyse impact of anomaly loss on transmission performance in systems with hybrid EDFA/Raman amplification and propose two mitigation techniques to minimize the impairment. We demonstrate that equalizing SNR_{ASE} provides better impairment mitigation than equalizing output power for the affected span in transmission link. ©2022 The Author(s)*

Introduction

We report a novel study on impact of anomaly loss on transmission performance and mitigation of its impairment in coherent optical transmission systems. There are increasing reports on monitoring and anomaly detection technologies in optical transmission link as we are adding intelligence in optical networks. Recently, anomaly detection based on signal processing technology in coherent optical communications has been reported that does not require any additional hardware, which is enabled by the property that nonlinear interference noise accumulation depends on dispersion and longitudinal power profiles in transmission links [1-4]. [1] reported power profile estimation (PPE) of multi-span transmission that enables anomaly detection and localization by evaluating correlation between intensity profile at transmitter and recovered intensity profile based on simplified digital back propagation. [2] and [3] reported PPE using neural network based digital-back propagation and Volterra nonlinear equalizer respectively. [4] showed PPE in optical links with remote optically pumped amplifiers and Raman amplifications. However, there are few studies on the impact of localized anomaly loss and mitigation technologies in coherent optical communication systems. It might be possible to replace links that have anomaly loss, but it may not be always possible without interruption of service.

For the first time, we study the impact of anomaly loss and propose mitigation in coherent optical transmission links with hybrid EDFA/Raman amplifiers. Through simulations, we analyse ASE noise and nonlinear interference (NLI) noise depending on anomaly location and power profiles in optical fiber links. Based on insights from this analysis, we propose two different mitigation algorithms and analyse their mitigation performance.

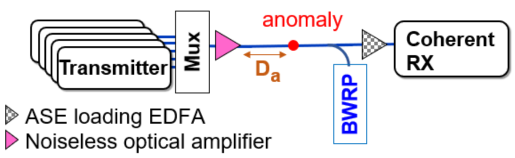

Fig. 1: Transmission system with hybrid Raman amplifier.

Methodology

To characterize the impact of anomaly, we study single span transmission of WDM channels with/without anomaly depending on location and attenuation over a fiber span with hybrid Raman amplifier, as shown in Fig.1. In the first step, intensity profile of WDM channels is calculated by solving coupled differential equations with boundary conditions as described in [5, 6]. In this study, backward Raman pump (BWRP) power is assumed to be un-depleted considering aggregate WDM signal power profile and BWRP power in transmission link. Thus, longitudinal power profile of BWRP is found first, then the ordinary differential equation is solved for forward propagation [6]. In second step, WDM signal is transmitted with split-step Fourier method to find NLI noise where longitudinal power profile of each channel follows the calculated profile in the first step. ASE noise from Raman amplifier (amplified spontaneous Raman scattering [5]) and EDFA is calculated, then added in SNR calculations.

Transmission system

Span length of transmission link is 150 km. Five 56 GBaud DP-64QAM channels with channel spacing of 75 GHz are transmitted over standard single mode fiber with hybrid Raman amplifier (Fig. 1). Root raised cosine filter with roll off factor of 0.15 is used. The fiber attenuation profile and Raman gain profile from [6] were used. Dispersion and dispersion slopes are 16 ps/nm/km and 0.057 ps/nm^2/km at 1552.5 nm that corresponds to the center wavelength of WDM signal. The effective length (L_{eff}) of nonlinear fiber is about 21.7 km. Nonlinear coefficient of fiber is 1.3 /W/km. Raman pump wavelength is 1452.9 nm such that the maximum

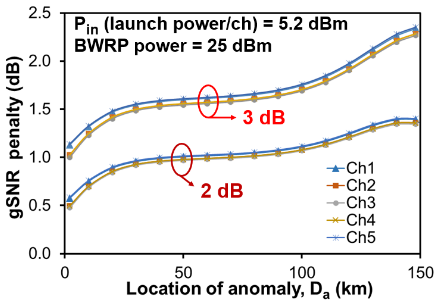

Fig. 2: gSNR penalty versus location of anomaly loss.

Raman gain corresponds to the wavelength of center channel. Noise figure of EDFA is set as 5.5 dB. EDFA is located at the end of span and Raman pump is launched from the end of span for distributed backward Raman amplification. Location of anomaly, D_a, is measured from the beginning of span where D_a = {2 km,10 km, 20 km, …,140 km,148 km}. The amount of anomaly loss is 2 dB or 3 dB in our simulation. As a performance metric for coherent communication systems, generalized SNR (gSNR) is evaluated as $(1/SNR_{ASE} + 1/SNR_{NLI})^{-1}$ where SNR_{ASE} is SNR with respect to ASE noise (EDFA and Raman) and SNR_{NLI} is SNR with respect to NLI noise [6, 7]. It is assumed that there is no implementation penalty in transponder systems.

Results I: Impact of anomaly

Figure 2 shows gSNR penalty in a single span transmission of WDM channels depending on the location and loss of anomaly compared to gSNR without anomaly. The optimal launch power is 5.2 dBm per channel for fiber link without anomaly when BWRP power is set as 25 dBm. There are two different groups of graphs depending on anomaly loss, 2 dB and 3 dB. 3 dB loss shows larger penalty than 2 dB loss as expected. In both groups, penalty increases as location of anomaly is closer to the end of span. To further understand the anomaly impact, SNR_{ASE} and SNR_{LNI} are plotted depending on the location of 2 dB anomaly loss in Fig. 3. SNR_{ASE} does not simply decrease by 2 dB due to BWRP compared to transmission without anomaly. However, SNR_{ASE} shows rather flat profile up to D_a ~ 100 km, and it starts to decrease as anomaly location is getting closer to the end of span. SNR_{ASE} decreases up to about 2 dB (red arrow), comparable to anomaly

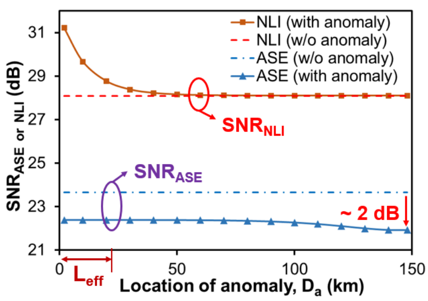

Fig. 3: SNR_{ASE} and SNR_{NLI} depending on anomaly location.

loss, when the location is very close to the end of span. In contrast to SNR_{ASE}, SNR_{NLI} is higher when the location of anomaly is close to the beginning of span, and it is asymptotically approaching the SNR_{NLI} of the case without anomaly as the location is getting closer to the end of span because most of NLI noise accumulation occurs in the effective length.

Proposed mitigation algorithms

SNR_{NLI} does not change that much if D_a is larger than the effective length (L_{eff}) as shown in Fig. 3, which means there is no need to reoptimize launch power if D_a is much larger than L_{eff}. Furthermore, we can expect degraded SNR_{ASE} can be improved by reoptimizing BWRP power. Thus, we propose two algorithms: output power equalization algorithm (PEA) and SNR_{ASE} equalization algorithm (SEA), to reoptimize launch power and BWRP power. The algorithms evaluate the center channel for reoptimization. *Output power equalization algorithm (PEA)*: If D_a < $2*L_{eff}$, then reoptimize launch power, otherwise launch power will not be adjusted and it will be the optimal launch power found without anomaly. Then, boost BWRP power till the output power from the span becomes comparable to that without anomaly. Thereby equalizing output power from span to the case without anomaly. *SNR_{ASE} equalization algorithm (SEA)*: Launch power reoptimization is same as PEA. In reoptimization of BWRP power, it will be boosted till SNR_{ASE} becomes comparable to the case without anomaly. In this case, we equalize SNR_{ASE} in hybrid Raman amplified span to the case without anomaly.

Results II: Mitigation of impact of anomaly

Figure 4 shows measured gSNR of center channel depending on the location of anomaly and mitigation algorithms. Dashed-red line is reference gSNR when there is no anomaly in fiber link with optimal launch power and BWRP power of 25 dBm. Measured gSNR with 3 dB anomaly loss shows the worst performance. gSNR reoptimization of launch power and BWRP power with PEA shows improved performance. Yet, the penalty due to anomaly can reach up to

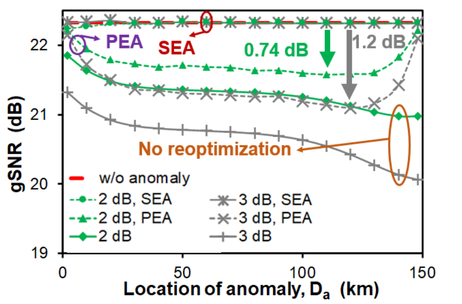

Fig. 4: gSNR depending on location of anomaly loss and mitigation algorithm.

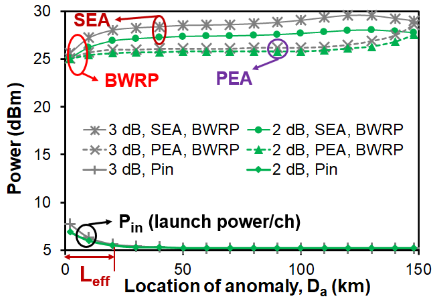

Fig. 5: Fiber launch power and BWRP power depending on reoptimization algorithm and location of anomaly loss.

0.74 dB and 1.2 dB for 2 dB and 3 dB anomaly loss respectively. On the other hand, when SEA is used, the gSNR is almost comparable to that without anomaly loss for both 2 dB and 3 dB loss irrespective of the location of anomaly. To understand the difference between these two algorithms, optimal launch power and BWRP power are plotted in Fig. 5.

Optimal launch power per channel is the same for both algorithms (PEA and SEA). The optimal launch power is higher as the location of anomaly is closer to the beginning of span while it is getting closer to 5.2 dBm as the location is beyond effective length, because most NLI noise accumulation occurs in the effective length. Meanwhile, the optimal BWRP power is clearly higher with SEA than PEA except at two locations of anomaly. If the anomaly is located close to the beginning of span, BWRP power is close to 25 dBm, while P_{in} is increased just to compensate loss. If the anomaly is located close to the end of span, then increased BWRP power with PEA and SEA are comparable. In this case, compensating decreased output power by anomaly (or equalizing output power) is also equalizing SNR_{ASE}. For further understanding, we just pick a location of anomaly and plot power profiles, gSNR and each component of SNR (i.e., ASE and NLI noise) for each algorithm.

Figure 6(a) shows the power profiles for three cases when there is no anomaly and anomaly with PEA or SEA (D_a = 30 km with 3 dB loss). We expect most NLI noise accumulation will be comparable in all cases because the power profiles are comparable in effective length. With regards to output power from the span, SEA shows the highest output power while the other 2 cases show comparable output power, which is expected because BWRP power is higher with SEA than PEA as in Fig. 5. However, the gSNR of all channels shows similar performance between transmission without anomaly and with SEA for anomaly mitigation in Fig. 6 (b). Each SNR component for gSNR calculation is also plotted in Fig. 6(c). Figure 6(c) shows that the SNR_{NLI} are comparable for all three cases as expected. Here, SNR_{NLI} is the worst in the center channel because of XPM from neighbouring channels. SNR_{ASE} is the worst when the launch power is reoptimized with PEA because ASE noise in Raman scattering is increased due to anomaly loss even though output power is equalized with PEA. In more detail, $SNR_{ASE\text{-}EDFA}$ (SNR calculated with respect to ASE noise from EDFA) is expected to be comparable when output power from span is equalized. However, $SNR_{ASE\text{-}Raman}$ (SNR calculated with respect ASE noise from Raman) is worse with PEA. Therefore, $SNR_{ASE} = (1/SNR_{ASE\text{-}EDFA} + 1/SNR_{ASE\text{-}Raman})^{-1}$ is decreased with PEA. Meanwhile, SEA further increases Raman pump power to equalize SNR_{ASE}. As a result, SEA equalizes gSNR because SNR_{ASE} and SNR_{NLI} with SEA are comparable to that without anomaly. In summary, ASE noise contribution from spontaneous Raman scattering is affected by anomaly. Thus, equalizing SNR_{ASE} provides better results than equalizing output power from span and achieves effective mitigation of anomaly. In addition, the proposed mitigation algorithms can be applied to a span with anomaly in multi-span transmission systems.

Conclusion

We analysed the impact of anomaly loss in coherent optical transmission link depending on loss and location for the first time. We proposed and evaluated two different mitigation algorithms for optical link with anomaly, which enables re-optimization of transmission link with minimal interruption of service. We demonstrated that, compared to PEA (equalizing output power), the SEA (equalizing SNR_{ASE}) can almost completely mitigate the impact of anomaly loss. It is envisioned that closed-loop autonomous operation of optical networks can be realized by combining anomaly detection, localization and mitigation techniques.

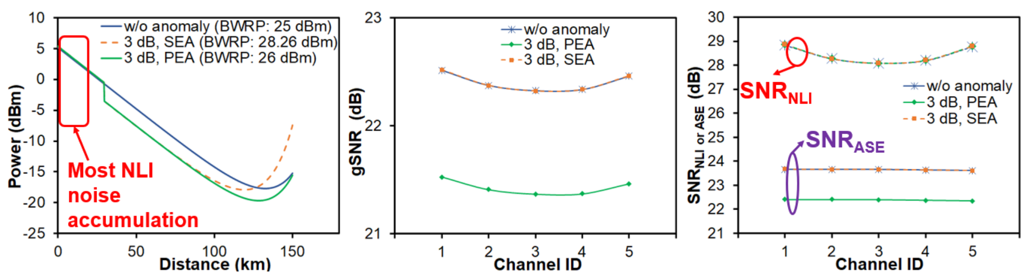

Fig. 6: (a) Power profile in fiber, (b) gSNR, (c) SNR_{NLI} and SNR_{ASE}.

References

[1] T. Tanimura, S. Yoshida, K. Tajima, S. Oda, and T. Hoshida, “Fiber-Longitudinal Anomaly Position Identification Over Multi-Span Transmission Link Out of Receiver-end Signals,” *Journal of Lightwave Technology*, vol. 38, no. 9, pp. 2726-2733, 2020. DOI:10.1109/JLT.2020.2984270.

[2] T. Sasai, M. Nakamura, S. Okamoto, F. Hamaoka, S. Yamamoto, E. Yamazaki, A. Matsushita, H. Nishizawa, and Y. Kisaka, "Simultaneous Detection of Anomaly Points and Fiber types in Multi-span Transmission Links Only by Receiver-side Digital Signal Processing," *Optical Fiber Communications Conference and Exhibition (OFC)*, San Diego, USA, 2020. DOI:10.1364/OFC.2020.Th1F.1.

[3] S. Gleb, P. Konstantin, J. Luo, and B. Zheng, "Fiber Link Anomaly Detection and Estimation Based on Signal Nonlinearity," *European Conference on Optical Communication (ECOC)*, Bordeaux, France, 2021. DOI:10.1109/ECOC52684.2021.9606094.

[4] L. S. Schanner, J. H. da Cruz Júnior, T. Sutili, and R. C. Figueiredo, "Power Profile Estimation of Optical Transmission Links based on Machine Learning," *IEEE Photonics Technology Letters*, vol. 33, no. 19, pp. 1089 - 1092, 2021. DOI:10.1109/LPT.2021.3104508.

[5] V. E. Perlin and H. G. Winful, "On Distributed Raman Amplification for Ultrabroad-Band Long-Haul WDM Systems," *Journal of Lightwave Technology*, vol. 20, no. 3, pp. 409 – 416, 2002. DOI:10.1109/50.988989.

[6] M. R. Zefreh, F. Forghieri, S. Piciaccia, and P. Poggiolini, "A Closed-Form Nonlinearity Model for Forward-Raman-Amplified WDM Optical Links," *Optical Fiber Communications Conference and Exhibition (OFC)*, San Francisco, USA, 2021. DOI:10.1364/OFC.2021.M5C.1.

[7] M. Filer, M. Cantono, A. Ferrari, G. Grammel, G. Galimberti, and V. Curri, “Multi-vendor Experimental Validation of an Open Source QoT Estimator for Optical Networks,” *Journal of Lightwave Technology*, vol. 36, no. 15, pp. 3073–3082, 2018. DOI:10.1109/JLT.2018.2818406.